Astron. Astrophys. 315, L32–L37 (1996)

ASTRONOMY
AND
ASTROPHYSICS

ISOCAM in flight⋆

C.J. Cesarsky[1], A. Abergel[2], P. Agnèse[1,3], B. Altieri[4], J.L. Auguères[1], H. Aussel[1], A. Biviano[4], J. Blommaert[4], J.F. Bonnal[1], F. Bortoletto[5], O. Boulade[1], F. Boulanger[2], S. Cazes†[2], D.A. Cesarsky[2], A. Chedin[6], A. Claret[1], M. Combes[7], J. Crétolle[1], J.K. Davies[8], F.X. Désert[2], D. Elbaz[1], J.J. Engelmann[1], G. Epstein[7], A. Franceschini[5], P. Gallais[1,4], R. Gastaud[1], M. Gorisse[1], S. Guest[4], T. Hawarden[8], D. Imbault[1], M. Kleczewski[1], F. Lacombe[7], D. Landriu[1], J. Lapègue[1], P. Léna[7], M.S. Longair[9], R. Mandolesi[10], L. Metcalfe[4], N. Mosquet[2], L. Nordh[11], K. Okumura[4], S. Ott[4], M. Pérault[2], F. Perrier[7], P. Persi[12], P. Puget[7], T. Purkins[8], Y. Rio[1], T. Robert[1], D. Rouan[7], A. Roy[1], O. Saint-Pé[7], J. Sam Lone[1], A. Sargent[13], M. Sauvage[1], F. Sibille[14], R. Siebenmorgen[4], F. Sirou[6], A. Soufflot[2], J.L. Starck[1], D. Tiphène[7], D. Tran[1], G. Ventura[10], L. Vigroux[1], F. Vivares[2], and R. Wade[8]

[1] Service d'Astrophysique/DAPNIA/DSM, CEA-Saclay, F-91191 Gif-sur-Yvette, France
[2] Institut d'Astrophysique Spatiale, F-91405 Orsay, France
[3] LIR/LETI, CEA-Grenoble, F-38054 Grenoble, France
[4] ESA/Villafranca Satellite Tracking Station, Apartado 50727, E-28080 Madrid, Spain
[5] Osservatorio Astronomico di Padova, I-35122 Padova, Italy
[6] Laboratoire de Météorologie Dynamique, F-91128 Palaiseau, France
[7] Observatoire de Paris, F-75014 Paris, France
[8] Royal Observatory, Edinburgh EH93HJ, Scotland
[9] Cavendish Laboratory, Cambridge CB30HE, UK
[10] Istituto di Tecnologie e Studio delle Radiazioni Extraterrestri, I-40129 Bologna, Italy
[11] Stockholm Observatory, S-13336 Saltsjöbaden, Sweden
[12] Istituto di Astrofisica Spaziale, I-00044 Frascati, Italy
[13] California Institute of Technology, Pasadena 91125, USA
[14] Observatoire de Lyon, F-69561 Saint Genis Laval, France

Received 6 September 1996 / Accepted 13 September 1996

Abstract. ISOCAM, the camera on–board ISO, takes images of the sky in the wavelength range 2.5 to 18 μm. It features two independent channels, containing each a 32×32 pixel detector: the short wavelength channel – 2.5 to 5.5 μm, and the long wavelength channel – 4 to 18 μm. Each channel features 10 or 11 discrete band pass filters and CVFs with a resolution better than 35. Each channel is fitted with a set of lenses, which reimage the focal plane of the telescope on the array, yielding a pixel field of view of 1.5, 3, 6 or 12 arcsec. Throughout the development cycle, ISOCAM has been carefully calibrated, first at component level and next at instrument level. The detectors have been thoroughly tested, including exposure to gamma rays and to fast protons and nuclei. The in-flight performance of ISOCAM matches all the expectations: for instance at 15μm and 6 arcsec field of view, 200 μJy sources are detected at the 10 σ level in 200 seconds.

Key words: camera – infrared – space

Send offprint requests to: cesarsky@cea.fr

⋆ Based on observations with ISO, an ESA project with instruments funded by ESA Member States (especially the PI countries: France, Germany, the Netherlands and the United Kingdom) and with participation of ISAS and NASA.

1. Introduction

In 1983, just as the first results of IRAS were presented to the European astronomical community, the decision was taken at the European Space Agency to fly a second generation infrared cryogenic satellite, ISO (the Infrared Space Observatory, see Kessler et al., 1996). While IRAS had scanned the whole sky in four colours, ISO was destined to do detailed studies of selected regions, with better angular resolution, wider wavelength coverage, enhanced imaging and spectroscopic capabilities, and a higher sensitivity. One of the four instruments was to be a camera, ISOCAM, the first astronomical space infrared camera with array detectors. After two years of design, seven years of development, test and calibration of the hardware, three years of completion of the software, now, in 1996, the first scientific results obtained with ISOCAM become available. The development of the hardware for ISOCAM, mainly funded by the Centre National d'Etudes Spatiales and the Commissariat à l'Energie Atomique, has involved over 150 scientists, engineers and technicians. Table 1 lists the hardware responsibility share among the laboratories.

The flight model was delivered to ESA in the first half of 1993 (Cesarsky et al., 1994). The software team continued com-

Table 1. ISOCAM Hardware Responsibilities

SAp–Saclay
Principal Investigator C.J. Cesarsky
Project Manager D. Imbault
System Engineer L. Vigroux
Management
Long wave detector and readout electronics
Instrument command electronics
Meudon Observatory
Short wave detector and readout electronics
Internal calibration device
IAS Orsay
Integration and calibration facility
R.O.E. Edinburgh
Optical concept, optical components
Stockholm Observatory
Filters
Italian laboratories
(TESRE, Padova Observatory)
Equipment for ground support equipment
and for observatory ground segment
The optical bench was subcontracted to Aérospatiale
The SW detector was manufactured by the
Société Anonyme de Télécommunications
The LW detector was manufactured by the
LIR/LETI/CEA Grenoble

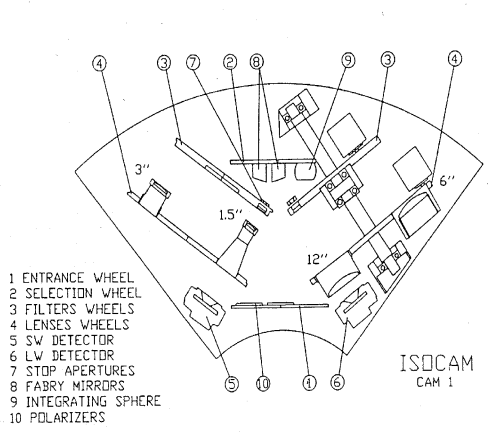

Fig. 1. Schematic lay-out of the IR camera, ISOCAM. The optical beam enters in the camera through the entrance wheel and can be directed to a short or a long wavelength channel by field mirrors fixed on the selection wheel. Each channel includes a filter wheel and a lens wheel.

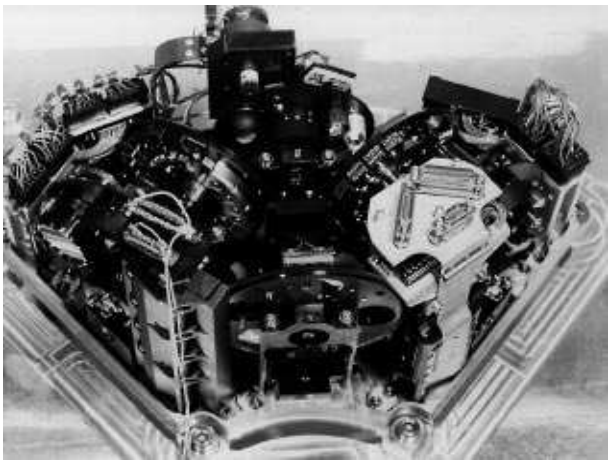

Fig. 2. Focal plane unit of the ISOCAM flight model

pleting its task, with a continuously enhanced contribution from ESA personnel. In 1994, the CAM Instrument Dedicated Team was created; since then, in close collaboration with the CAM Support Team, it has been responsible for a large number of tasks in preparation for the launch, as well as for the scientific monitoring of the instrument and of its calibration during the mission.

2. ISOCAM characteristics

ISOCAM (fig. 1 and 2) is a two channel camera, featuring two (32 × 32) pixel detectors, one for short wavelengths, SW: 2.5 to 5.5 μm, the other for long wavelengths, LW: 4 to 18 μm. On each channel, there are two wheels, one wheel holds four lenses, allowing four different pixel fields of view (1.5, 3, 6, and 12 arcsec.); the other holds 10 to 11 fixed filters and one (SW) or two (LW) Continuous Variable Filters (CVF), allowing to reach a spectral resolution of better than 35. The entrance wheel has five positions: 3 polarizers and 2 holes. The selection wheel holds Fabry mirrors which can either direct the light beam of the ISO telescope towards one or the other of the detectors, or can illuminate them uniformly with an internal calibration source for flat field purposes. ISOCAM is composed of 4 units :

(a) A 10 kg opto-mechanical unit, implemented at 3K in the focal plane of the telescope, including 2 detectors and 6 wheels on which are mounted the optical components and the internal calibration device.

(b) A 2 kg pre-amplifier unit, fitted to the external wall of the cryovessel as close as possible to the detectors, and working at 130K.

(c) Two 6 kg electronics units, implemented on the satellite service module, for instrument control and transmission to the ground of up to one 32 × 32 image every 2 seconds.

Much development work was necessary for the focal plane unit which had to satisfy stringent constraints : reliable operations at a temperature as low as 2.4 K, positional accuracy of typically 100 microns, angular accuracy in the milliradian range, a mean thermal dissipation lower than 10mW with peak dissipation below 50 mW. We briefly describe some of the solutions adopted.

2.1. Cryomechanisms

The ISOCAM mechanisms must withstand difficult constraints: cryogenic temperatures, high reliability, low dissipation, and good positioning accuracy. Of course, they had to survive the high level of vibrations during launch. To save development

time, we based the design of these mechanisms around a superconductor stepper motor developed by SAGEM which was already space qualified. We developed the gear train and the pinion required to adapt this motor to our needs. Positional encoding of each wheel is obtained thanks to three magnetoresistive devices (Sirou et al. 1989).

2.2. Optics

A very simple optical design has been adopted: the ISO telescope image is reimaged on the detector with a single aspherized relay lens. The beam is folded by a spherical field mirror, which is also used as a field diaphragm. The pupil size is 2.6 mm. The mirrors are made of Aluminium while the lenses are of Silicon (SW) and Germanium (LW). All optical components have been diamond turned, by Ferranti Astron in UK for the Qualification Model components, and by SOPELEM in France, for the flight model. The filters and the CVF are located near the pupil plane. The filters have been manufactured by SPECTROGON, under the supervision of the Stockholm Observatory, which has verified that they adequately block the light out of their specified range. The CVF have been manufactured by OCLI. All optical components have been measured in the ISOCAM test facility at the Royal Observatory of Edinburgh after they had been mounted in their holders by Aérospatiale. The filters are tilted by 5 deg, to avoid ghosts due to reflections between the filters and the detectors. Mounting the CVFs, which have very fragile substrates, was a particularly difficult task, and it was not possible to tilt them.

The focal plane unit of ISOCAM (Fig. 2) was built by Aérospatiale. The overall optical performance was tested in a special purpose facility in the Cannes plant using Si:Ga detectors arranged in the shape of a cross. These tests also allowed to determine the position at which the array detectors had to be placed. The fully integrated camera was characterized at the Institut d'Astrophysique Spatiale, Orsay, in the ISOCAL facility designed for this purpose.

Overall, the image quality results of the flight model (Vigroux et al. 1993, Pérault et al. 1994, Boulade et al. 1995) showed good agreement with expectations, confirming that Aérospatiale had succeeded in satisfying the tight wheel positioning specifications and that the opto-mechanical design of ISOCAM was sound and robust.

2.3. The Long Wavelength detector

At the time of the ESA Call for Proposals, there was no detector available in Europe for the LW channel, and it was not possible to import American detectors. A specific development was undertaken at the Laboratoire d'Infrarouge of LETI, in CEA-Grenoble. It is a photoconductor array in Si:Ga hybridized by indium bumps to a direct voltage readout circuit. It has 32×32 pixels, a 100 μm pitch and a thickness of 500 μm. Despite the absence of a front grid, this detector has a very low optical crosstalk. For the fastest lens of the camera, the 12 arcsec. lens which has a numerical aperture of f/0.6, the optical crosstalk remains below 1.5%.

The readout circuit has an integration capacitance of 0.12pF and a MOS follower with a gain of 0.8. Recommended individual integration times in flight are between 0.28 and 10 seconds. The noise characteristics of this system, as measured on ground, present several components: a high frequency term which is well approximated by a constant readout noise of some 180 $e^-/pixel$ and photon shot noise, and a low frequency noise which becomes important after roughly 50 readouts. At high level, $\geq 10^6 e^-/pixel$, the amplifier noise becomes preponderant and limits the S/N ratio to around 500 in a single image (Agnèse et al. 1989).

Extensive tests in laboratory, and then on the integrated camera, showed that this detector has some very good characteristics: high sensitivity, stable dark and flat fields, good resistance to high energy radiation (Agnèse et al. 1991). Its main drawback is a time-lagged response after a flux step, either up or down. This transient has to be taken into account when preparing the observations by allowing always a number of stabilization read-outs at the beginning of every observation. Typical stabilization times needed to achieve a flat field stable to within 1%, or a photometric response to within 10% of the flux step, range from three to several hundred single exposures (cf. the ISOCAM Observer's Manual, 1994, hereafter IOM). To extract *all* the information from the data, it is necessary to use models of the transients. In some rare cases the hits from high energy particles (glitches) induce responsivity variations whose effects have to be considered.

The flat fielding accuracy can be as good as $5.0\ 10^{-3}$ when the detector is stabilized. The flat field stability allows the use of a flat field library. However, a limitation comes from the differential stabilization times between pixels in the array, which can be quite long. A good way to remove these small effects, as well as the low frequency noise mentioned earlier (which in fact may be related to these effects), is to resource to a beam switching strategy. Alternatively, a microscanning procedure can be used, displacing the detector by a few arc seconds on the sky every few exposures; this can be realised using the raster pointing mode of ISO.

2.4. The Short Wavelength detector

For the SW channel, the basic device is a 32×32 pixels CID InSb array manufactured by the Société Anonyme de Télécommunications. At the time of ISOCAM selection, this detector was already space qualified and had the advantages of a low operating temperature and a large radiation tolerance, compatible with the ISO mission. Several upgrades of the existing devices have been made : increase of the pixel pitch up to 100 μm, increment of the surface filling factor to 89%, and a new design of the supporting ceramic to reduce electrical cross talk. Control and readout hybrid electronic were designed to work at 4K close to the chip (Tiphène et al. 1989).

Measurements of the pixel charge can be done by sensing the voltages of the 32 output lines and sequentially injecting the

pixel charges in the substrate through column voltage clocks. The analogue chain uses an adaptive filter followed by high gain preamplifiers. The output signal is nevertheless very small, a few μV, and the lines are very easily affected by pickup noise. To calibrate this noise, two blind lines were added in the detector and the electronics chain, for use as a reference for the correlated pickup noise. A correlation matrix can be determined between the pixels on the reference lines and the actual pixels, and used to remove the correlated noise. This procedure is very efficient. After subtraction of the correlated noise, the remaining noise can be very well modeled by a constant readout noise plus photon shot noise. The rms readout noise measured on the ground is 700 electrons/pixel. The charge generation in this detector, in the dark, is not due to thermal effects, but to tunnel effects. It increases only as the logarithm of the integration time, so that long integration times are possible without saturation. In addition, in this detector, the active zone of the pixel is very thin (less than 10 μm), so that it has a low susceptibility to radiation effects. It does not need to be cured after passing through the radiation belts, and glitches due to high energy particles are relatively infrequent and tend to affect only one pixel. This array also has a time lagged response after a flux step, and the observer has to allow for long enough stabilization times. The array has four low responsivity pixels, all close to the side of the array.

2.5. The Internal Calibration Device

The internal calibration device was designed to provide an internal flat field source, and a rough calibration reference. Calibration of the SW channel required sources near 350K which are difficult to fit in the low thermal dissipation allocation of ISO. We use a small resistor, $0.6mm^2$, mounted on a thin kapton film. This emitter feeds through a small input hole an integrating sphere which is mounted on the selection wheel. In the calibration mode, the output hole of the integrating sphere takes the place of the Fabry mirror. The temperature of the emitter can vary in the range 150 K to 350 K. The brightness uniformity is better than 3% in the unvignetted circular 3 arc minute field of view of ISO. This source is very stable: the reproducibility of calibrations remains within $\pm$3 %.

2.6. Electrical design

The electrical architecture is standard for a space experiment. It is organized around a 16 bit 80C86 microprocessor, powered by hybrid DC/DC converters using the satellite 28 volt power line. Redundancy is obtained by mounting two independent microprocessor units and DC/DC units which can be selected by external switches.

3. In flight performance versus expectations

An ISOCAM photometric model for all optical configurations had been established from individual component transmission curves plus a global rescaling (one coefficient each for LW and SW filters plus one coefficient each for SW and LW CVFs). The model was compared to measurements made on the flight model in the ISOCAL facility (Pérault et al., 1994). ISOCAL's extended source had been absolutely calibrated by comparison to a laboratory black-body. Filter and CVF discrepancies with respect to the photometry model had been found with amplitudes up to 30 %, but we were not convinced that introducing further refinements at pre-launch stage would be beneficial. The point source calibration was derived from the extended source calibration, assuming 100 % of the flux is collected in the diffraction pattern allowing us to draw curves for the expected sensitivities to extended and point sources. Examples taken from the IOM are shown in figures 4 and 5.

3.1. Missing column of the LW detector.

The first tests of ISOCAM, after launch and before ejection of the cryocover, revealed that column 24 of the LW detector is disconnected. Tests on the ground, during the thermal vacuum test of ISO, had already detected this problem, which was tentatively attributed to a faulty connection at the feedthrough connector level, but unfortunately on the internal side of the cryovessel. The problem was not judged important enough to justify extensive investigations which would have delayed the launch.

3.2. Effect of high energy particles on the LW detector

ISO's launch coincided with the beginning of a solar minimum activity period. The flux of galactic cosmic rays is then enhanced, compared to the IOM estimate which corresponded to a solar maximum period. Using the data provided by the KET instrument on board of Ulysses (P. Ferrando, 1996) when it crossed the ecliptic plane, we derive the following rates of cosmic ray hits on the array: 0.28 protons (E $\geq$ 30 MeV)/s and 0.2 alpha particles (E $\geq$ 30 MeV)/s. The IOM pre-flight modelling also ignored the role of secondary particles (mainly electrons, created by interactions of primary particles with matter in the neighbourhood of the detector) which in fact doubles the total rate of events and accounts for the large proportion of cases where only a few pixels are affected.

Very effective deglitching algorithms have been developed. They are implemented, in order of increasing sophistication, in the Auto Analysis and Interactive Analysis software packages. A short description of these procedures is given in the ISOCAM Data User Manual. At present, the best results are obtained with the Multiresolution Median Transform method (Starck et al. 1996a).

During ISO's passage in the radiation belts, the LW detector remains switched on, and the optical configuration is such that the detector is always illuminated. The residual photocurrent in this configuration is sufficient to drag most of the charges created by the charged particles in the detector. Simulations on ground had indicated that this perigee mode should be adequate to prevent a large increase in responsivity at the end of the belt crossing, and this was indeed verified in flight. Consequently,

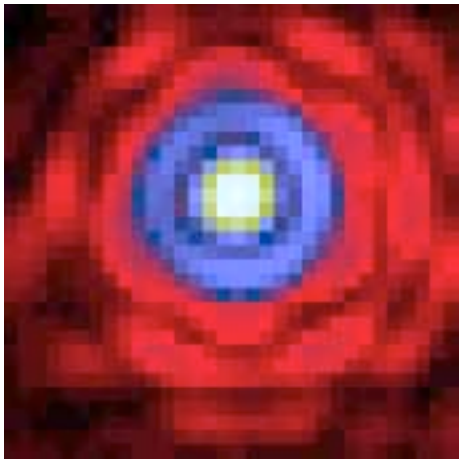

Fig. 3. Observed ISOCAM PSF at 15 μm. The logarithmic scale allows to visualize the diffraction pattern down to the 4^{th} Airy ring. The 5^{th} ring can be detected on deeper images. One pixel equals 1.5 arcsec and the diameter of the first dark ring is $\sim$ 12 arcsec, as expected.

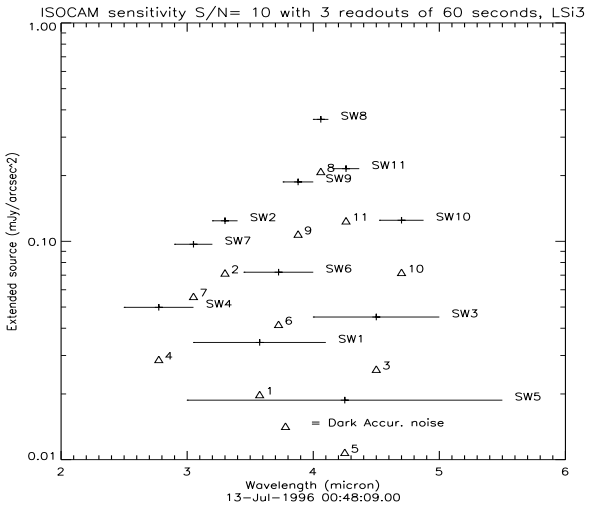

Fig. 4. Extended source flux giving a signal to noise ratio of 10 for all SW filters, for 3 individual integration of 60s, and a 3 arsec. pixel field of view (corrected from the ISOCAM Observer's Manual; see text).

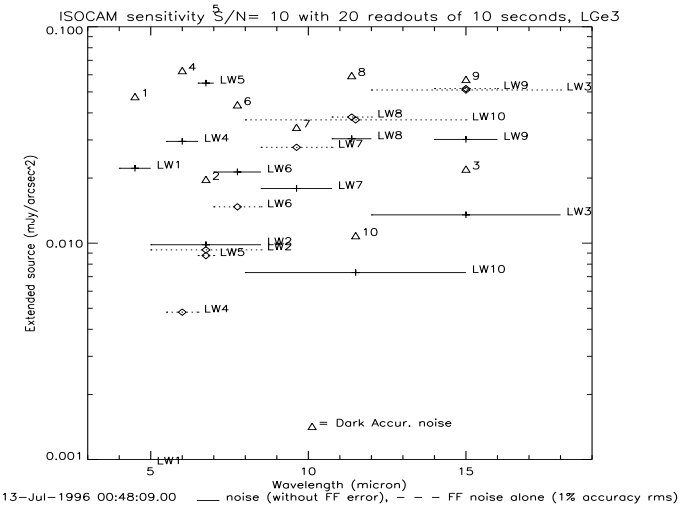

Fig. 5. Same as figure 4 but for all LW filters, for 20 individual integration of 10s. The assumed flat field accuracy is 10^{-2}, for a zodiacal background comparable to its level at the pole.

ISOCAM does not require a detector curing phase at the start of the "science" part of the orbit.

3.3. Transients

The transients on the detectors are as expected; cf. IOM. In principle, source detection can be obtained rapidly, since the signal, when reaching a source, raises very rapidly to 60% of its final value; however, several exposures are necessary to tell glitches from sources and to obtain good photometry.

3.4. Image quality

To measure the ISOCAM Point Spread Function (PSF) we have performed, with various filters, micro-scan rasters with 6 displacements of 2 arcsec. in each direction, 400 images at each position, using a pixel field of view of 1.5 arsec. Figure 3 shows the PSF measured, obtained after registration of each image to correct for the pointing jitter. The agreement with the theoretical PSF is very good, with the Airy pattern well reproduced up to the fourth ring.

3.5. Sensitivity

The photometric calibration of ISOCAM is still ongoing, and detailed results will be presented elsewhere. Still, the results obtained up to now allow us to make a first assessment of our spectro-photometric model of the camera. This is based on photometry on 6 calibration stars, and on the zodiacal background, using as reference the results obtained by DIRBE, onboard the COBE satellite (see Reach et al. 1996). Few discrepancies have been found between the model and the performances measured in flight:

(1) Point sources in the LW channel systematically appear a factor 0.7 to 0.8 fainter than expected, while extended sources (namely the zodiacal background) give measured brightness in excellent agreement with the expectations. Part of this discrepancy may be due to straylight contamination of extended sources, The issue will be investigated by means of specific meaurements to be scheduled as part of the ISOCAM calibration strategy.

(2) A known but overlooked error in the photometric estimates used for the IOM led to an underestimation of the sensitivity of the SW channel shortwards of 3.5 μm by up to 50%; this has been corrected in figure 4. Apart from this mistake, measurements of point sources in the SW broad band filters show that the sensitivity of the SW detector is 20% higher than expected.

(3) For the CVFs, results in flight confirmed the accuracy of the spectral calibration. The detailed spectral response of the

LW CVFs, derived from stellar observations, differs from the tables in the IOM by up to 20% at some wavelengths. For point sources, a further correction factor of 0.67 should be applied. For the SW CVF, the results are still under analysis.

3.6. Faint point source detection.

The extraction of point sources of flux below 1 mJy from the data is cumbersome, because of the combined effect of the glitches and of the memory effects. Several methods are under development to tackle this problem. A method devised by Starck et al. (1996b), based on repeated studies of the temporal variation of the signal of each pixel, has allowed the detection of sources whose brightness, in a band around 6.75 μm, is presently estimated to be as low as 60 μJy (Pierre et al., 1996).

4. Conclusion

The performance of ISOCAM in flight matches the expectations: apart from the loss of one column in the LW detector, the behaviour of the camera is as expected. It is yielding, for the first time, detailed maps of the sky in the 2.5 to 18 μm wavelength range whose interest had been highlighted 13 years ago by IRAS, but with an angular resolution which can be 50 times better, a sensitivity 1000 times higher, access to the whole wavelength range and the possibility of performing spectral maps and of obtaining spectra of very faint extended sources. The first scientific results of ISOCAM, presented in this issue, witness to the large potential for interesting science to be expected from the ISO mission.

References

Agnèse, P., Lucas, C., Maillart, P. et al., 1989, SPIE, 1070, 124
Agnèse, P., Engelmann,J.J., Mottier, P., 1991, IEEE Transactions on Nuclear Science, 38, 953
Boulade, O., Cesarsky, C.J., Crétolle, J. et al., 1995, SPIE, 2475, 360
Cesarsky, C.J., Bonnal, J.F., Boulade, O. et al., 1994, Optical Engineering, 33, 751
Ferrando, P., personal communication
Kessler, M.F. et al., 1996, *this volume*
Pérault, M., Désert, F.X., Abergel, A. et al., 1994, Optical Engineering, 33, 762
ISOCAM Observer's Manual, 1994. The ISOCAM Team and A. Heske. *Available with the ISO Documentation.*
Pierre, M. et al., 1996, *this volume*
Reach, W. et al., 1996, *this volume*
Sirou, F., Gillet, B., Glaise, R. et al., 1989, Cryogenics, 29, 883
Starck, J.L., Claret, A., Siebenmorgen, R., 1996a, SAP technical report
Starck, J.L., Aussel, H., Elbaz, D., 1996b, SAP technical report
Tiphène, D., Rouan, D., Lacombe, F. et al., 1989, "Infrared Astronomy with Arrays", Univ. of Hawaii, G. Wynn Williams and E. Becklin ed., p. 237
sert, F.X.,
Vigroux, L., Cesarsky, C.J., Boulade, O. et al., 1993, SPIE, 1946, 281